**Daniel J. Lunt · Nathalie de Noblet-Ducoudré
Sylvie Charbit**

Effects of a melted greenland ice sheet on climate, vegetation, and the cryosphere

Abstract This paper investigates the possible implications for the earth-system of a melting of the Greenland ice-sheet. Such a melting is a possible result of increased high latitude temperatures due to increasing anthropogenic greenhouse gas emissions. Using an atmosphere-ocean general circulation model (AOGCM), we investigate the effects of the removal of the ice sheet on atmospheric temperatures, circulation, and precipitation. We find that locally over Greenland, there is a warming associated directly with the altitude change in winter, and the altitude and albedo change in summer. Outside of Greenland, the largest signal is a cooling over the Barents sea in winter. We attribute this cooling to a decrease in poleward heat transport in the region due to changes to the time mean circulation and eddies, and interaction with sea-ice. The simulated climate is used to force a vegetation model and an ice-sheet model. We find that the Greenland climate in the absence of an ice sheet supports the growth of trees in southern Greenland, and grass in central Greenland. We find that the ice sheet is likely to regrow following a melting of the Greenland ice sheet, the subsequent rebound of its bedrock, and a return to present day atmospheric CO_2 concentrations. This regrowth is due to the high altitude bedrock in eastern Greenland which allows the growth of glaciers which develop into an ice sheet.

D. J. Lunt (✉) · N. de Noblet-Ducoudré · S. Charbit
Laboratoire des Science du Climat et de l'Environnement (LSCE),
Unite mixte de Recherche CEA-CNRS, Bat. 709/Orme des
Merisiers, 91191 Gif-sur-Yvette, France
E-mail: d.j.lunt@bristol.ac.uk
Tel.: +44-117-9288186
Fax: +44-117-9287878

Present address: D. J. Lunt
Bristol Research Initiative for the Dynamic Global Environment
(BRIDGE), School of Geographical Sciences,
University of Bristol, University Road, Bristol,
BS8 1SS, UK

1 Introduction

Present anthropogenic emissions of greenhouse gases into the atmosphere are leading to increased global mean surface temperatures (IPCC2001). Modelling studies, which examine the effects of the increase of such emissions, indicate that the greatest warming in the future is likely to be in high northern hemisphere latitudes, due to sea-ice and snow albedo feedbacks (IPCC 2001). These studies are typically run with coupled atmosphere-ocean general circulation models (AOGCMs), and simulate climate over a timescale of about a century. Over millenia timescales, it is likely that ice-sheet/climate feedbacks will be important in determining the evolution of future climate. Due to the long timescales involved, this is yet to be extensively investigated in the framework of an AOGCM. However, simpler earth system models of intermediate complexity (EMICs), can more easily be used to simulate climate over the timescales involved in ice-sheet/climate interactions. Loutre (1995) forced the LLN-2D EMIC, which includes relatively simple interactive ice sheets, with a plausible CO_2 concentration scenario for the next 5,000 years, peaking at 710 ppmv in year 500, and found that the Greenland ice sheet almost completely melted by the end of the simulation. More recently, Loutre and Kageyama (2003) forced the CLIMBER EMIC, coupled (via the atmosphere only) to a 3D ice sheet model, with another plausible CO_2 scenario peaking at over 1,600 ppmv in year 325 of the model simulation, and also arrived at an entirely melted Greenland in about 5,000 years. As well as a direct climatic effect, related to the decrease in altitude and change in surface characteristics, the melting of the Greenland ice-sheet would result in a sea-level rise of about 7 m, and possible changes to the thermohaline circulation, due to the input of freshwater. The climatic effect has been investigated by Toniazzo et al. (2004), who found a 6.7°C increase in annual mean surface air temperature over an ice-free Greenland,

relative to present, using an AOGCM. By examining the development of snow-cover over Greenland bedrock in the model, they also concluded that, given a return to pre-industrial CO_2 levels, the Greenland ice-sheet would not re-glaciate. However, they did point out the need for high-resolution ice-sheet model simulations to investigate this further. In the context of the Pliocene glaciation of Greenland, Crowley and Baum (1995) carried out a series of GCM sensitivity studies with an ice-free Greenland, and found that, with a variety of different prescribed surface types in the place of the Greenland ice sheet, the Greenland summer surface air temperature remained above 0 °C, and there was no build-up of snow cover in the model. They also suggested that even with a model capable of resolving the high-altitude mountains in eastern Greenland, an ice-sheet may not develop due to high summer temperatures at lower altitudes, enhanced by vegetation feedbacks.

In this paper, we investigate the effects on the earth system of a melting of the Greenland ice sheet. Using an AOGCM, we investigate the direct and indirect effects of the melting of Greenland on the atmosphere. In a similar way to previous workers (Rind 1987; Felzer et al. 1996), we look at the relative importance of albedo and ice-sheet height on determining the response to the change in boundary conditions. Focus is on the mean climatic effect of the removal of the ice sheet, rather than transient effects, such as its influence on individual cyclones, for which higher resolution models are more appropriate (Kristjánsson and McInnes 1999). As well as telling us about possible future climate changes, it also gives insight into the role of Greenland in influencing present day weather and climate. By feeding the climate, obtained in the AOGCM without the ice sheet, into an off-line vegetation model, we investigate the likely distribution of vegetation on an ice-free Greenland. Using a similar methodology with a high resolution ice-sheet model, we also address the question of whether the Greenland ice sheet is likely to re-glaciate, following a melting driven by greenhouse gas increases.

2 Experiment description

The results shown in this paper are primarily based on two AOGCM simulations: a present day control, and a simulation in which the Greenland ice sheet is removed. The results from the AOGCM simulations are then used to force an offline vegetation model, and an offline ice-sheet model. Section 3.1 describes the models, and Sect. 3.1 gives details of the simulations.

2.1 The models

To perform the two AOGCM simulations in this paper, we use the Institut Pierre Simon Laplace (IPSL) coupled ocean-atmosphere GCM, IPSLCM4. This model consists of the LMDz3.3 atmospheric model (Li 1999), the OPA8.1 ocean model (Madec et al. 1999), and the SECHIBA land surface scheme (Ducoudré et al. 1993; Viovy and de Noblet 1997; de Rosnay and Polcher 1998). For this work, the spatial resolution of LMDz3.3 and SECHIBA is 5° in longitude and 4° in latitude. That of OPA8.1 is 4° in longitude and 3° in latitude, with an increased latitudinal resolution of 1° near the equator. LMDz3.3 has 19 vertical levels, and OPA8.1 has 30, with a resolution of 10 m in the topmost 100 m, and 500 m near the bottom. Physical parameterisations in LMDz3.3 include the Tiedtke (1989) convection scheme and the Lott and Miller (1997) sub-gridscale orography scheme. Treatment of radiation follows Fouquart and Bonnel (1980) for short-wave radiation, and Morcrette (1991) for long-wave radiation. The OPA8.1 model solves an approximate form of the Navier-Stokes equations and the equation of state. Turbulent diffusion and viscosity are parametrized along neutral surfaces (surfaces along which fluid particles can be moved without doing any work against gravity), and vertically. The turbulent kinetic energy (TKE) scheme of Blanke and Delecluse (1993) is used in the vertical, to compute mixing coefficients. On neutral surfaces, the parametrization of baroclinic instabilities of Gent and McWilliams (1990) is used. Coupled to the ocean model is the LIM sea-ice model (Fichefet and Morales Maqueda 1999), which simulates salt, freshwater, and momentum exchanges between the ice and ocean. We use OPA8.1 in 'damped' mode, where the deep ocean temperatures and salinities are nudged towards those of present day observations (Levitus 1982), using a Newtonian damping term. This technique results in a shorter period for the system to reach equilibrium than in the fully coupled mode (years as opposed to centuries), but allows the upper ocean to interact thermodynamically with the atmosphere. However, the damping means that energy and salt are not strictly conserved, and the ocean current response to changes in forcing is not simulated correctly. The damping is not applied in the uppermost 100 m of the ocean, to allow sea surface temperatures (SSTs) and, in particular, sea-ice, to respond to changes in atmospheric forcing. Nor is it applied in the surface mixed layer, whose depth is diagnosed from the TKE scheme. In regions like the North Atlantic, this allows the ocean to rapidly react to atmosphere fluxes on depth of several hundred meters. A simulation we have carried out under increased CO_2 conditions, using the damped ocean, (Lunt and de Noblet-Ducoudré 2003) shows patterns in surface temperature change which more closely resemble those from fully coupled simulations (e.g. IPCC 2001) than from simulations using a slab ocean (e.g. IPCC 1995). Compared to the traditional slab ocean, our approach allows for more feedbacks between the ocean and the atmosphere. In a previous study similar to this one, in which fresh water fluxes associated with the melting of Greenland were also ignored, Toniazzo et al. (2004) used a fully coupled ocean model without any damping, but found no evidence of significant change in the strength of the Atlantic meridional overturning

circulation, which further justifies our use of the damped ocean.

For the vegetation simulations, we use ORCHIDEE, which is a dynamical global vegetation model, developed by Krinner et al. (Submitted to Global Biogeochemical Cycles). It is principally designed to be included on-line in atmospheric GCMs or regional climate models, but can also be used in off-line mode, where the atmospheric forcing is imposed from either observations or climate simulations. ORCHIDEE simulates the principal processes of the continental biosphere influencing the global carbon cycle (photosynthesis, autotrophic respiration of plants, and heterotrophic respiration from soils) as well as latent, sensible, and kinetic energy exchanges at the surface of soils and plants. As a dynamical vegetation model, it explicitly represents a number of competing processes (such as fighting for light), the response of plants to some disturbances such as fire, and the ability of plants to quickly colonize non-vegetated areas. It can thus be used in transient simulations of climate change. The whole seasonal phenological cycle is calculated prognostically without any prescribed dates or use of satellite data. One of the ORCHIDEE sub-models, SECHIBA (Ducoudré et al. 1993; Viovy and de Noblet 1997; de Rosnay and Polcher 1998), which computes all instantaneous fluxes at the land-surface/atmosphere interface, has been used on-line for the GCM simulations, while the full code has been used off-line to investigate the vegetation resulting from the GCM-simulated climates. The land-surface, in ORCHIDEE, is described as a mosaic of 12 plant functional types (PFTs) and bare soil. Each of these 13 surface descriptors can simultaneously occupy the same grid box. Fluxes and soil moisture reservoirs are computed separately for each PFT (and bare soil). High-latitude biomes are not represented, as such, in ORCHIDEE but may result, as in most global dynamic vegetation models, from combinations of our limited set of PFTs. The very large variations in the composition and structure of Artic ecosystems (for example erect versus prostrate dwarf shrub tudra, cushion forb, lichen and moss tundra), that are largely determined by specific climatic gradients (for example growing season warmth, soil moisture and snow cover), are obviously not very well represented in such models and the launch of initiatives like the pan arctic initiative (Kaplan et al. 2003) will lead to the improvement of ORCHIDEE-like models in the near future. Nevertheless, as our goal in this paper is to see whether the climatic conditions over an ice-free Greenland would allow for the growth of any type of vegetation, we think ORCHIDEE, even at these very high latitudes, is adapted for that purpose.

The ice sheet model used in the present work is the GREnoble model for land ice of the northern hemisphere (GREMLINS), developed in the Laboratoire de Glaciologie et de Geophysique de l'Environnement, Grenoble. The model has been calibrated against present-day Greenland. It is forced by surface temperature and precipitation data, which can either come from observations, such as CRU (New et al. 1999), or from model output, such as a GCM. A comprehensive description of the model and its equations can be found in Ritz et al (1997). The model is a three-dimensional thermomechanical ice-sheet model that predicts the evolution of the geometry (extension and thickness) of the ice and the coupled temperature and velocity fields. The model deals only with grounded ice and not with ice shelves. The equations are solved on a Cartesian grid (45×45 km) corresponding to 241×231 grid points in the Northern Hemisphere. The evolution of the ice sheet surface and geometry is a function of surface mass balance, velocity fields, and bedrock position. The isostatic adjustment of bedrock in response to the ice load is governed by two components: the flow of the asthenosphere with a characteristic time constant of 3,000 years, and the rigidity of the lithosphere which is taken into account by computing the spatial shape of the deflection due to one unit load. The temperature field is computed both in the ice and in the bedrock by solving a time-dependent heat equation. Changes in the ice thickness with time are a function of the ice flow, the surface mass balance and the basal melting. The ice flow results both from internal ice deformation and basal sliding, and the surface mass balance is the sum of accumulation and ablation. The accumulation term is computed from the GCM simulated precipitation, assuming that with a surface air temperature below 2°C, all the precipitation is solid precipitation (the value of 2°C is from an observational study carried out in the Alps by the Centre d'etudes de la neige, Grenoble (Catherine Ritz, personal communication)). The ablation term is computed using the positive degree day method which is based upon an empirical relation between air temperatures and melt processes.

2.2 The simulations

We carry out two simulations using the IPSLCM4 GCM. These are a present day control simulation (control), and a simulation in which the Greenland ice sheet is removed (noice). In the noice simulation, the orography in the Northern Hemisphere is taken to be that of the bedrock after isostatic rebound. After, and during a melting of the Greenland ice sheet, the bedrock would rebound upwards, no longer held down by the weight of the ice sheet. To assess this rebound for Greenland, we forced the GREMLINS ice sheet model with a very large surface heating and decrease in precipitation, so that the Greenland ice sheet completely melted. It is beyond the scope of this paper to investigate the melting in any detail, our objective being only to get a rebounded Greenland as a boundary condition for the noice simulation. Following the melting, the bedrock rebounded and equilibrated in about 4,000 years. The equilibrium bedrock height, which is independent of the speed of the melting, is the altitude used in the noice simulation. This is the same approach as used by

Toniazzo et al. (2004); in fact, they carried out two simulations, one with a rebounded topography and one without rebound, and did not find any major differences between them.

In addition to the orography change, the Northern Hemisphere ice sheets are replaced with a barren tundra vegetation. The principal effect of the change in surface type is a decrease in the albedo of the snow-free surface. There are also secondary changes related to the change in surface type: the surface roughness length over Greenland increases, water is allowed to moisten the soil, and fluxes such as transpiration, interception loss and evaporation of ground-water can take place, together with sublimation of snow.

No freshwater flux anomalies are applied in any of the simulations described in this paper; they are equilibrium simulations. In reality, accompanying the melting of an ice sheet such as Greenland, there would be a flux of fresh water into the surrounding oceans. This would potentially have effects on the stability of the thermohaline circulation. However, this flux is not applied in this GCM simulation because the damped ocean temperatures and salinities used in our simulations make the model incapable of correctly simulating fresh water flux anomalies. The freshwater flux problem is discussed further in Sect. 6. Our main assumption in this sensitivity study is that even if the fresh water flux results in a weakening of the thermohaline circulation, it is likely to eventually recover. Our GCM simulations therefore represent a time period after which equilibrium has been reached. We also neglect the approximately 7 m sealevel rise associated with the freshwater input. The sealevel rise would only affect a small number of gridboxes in the model simulation and is unimportant for global climate, but could have a large effect on coastal communities. We have chosen to keep CO_2 and other greenhouse gas concentrations the same as in the control simulation. This is primarily to allow a clean comparison between the two simulations. Also, our simulation can be thought of as representing a time period in the future when greenhouse gases have decreased from their maximum values, and reached present day values again. The scenario used in the CLIMBER simulation discussed in Sect. 2 suggests that this could be approximately 60,000 years in the future. At this time, the earth's orbit would be different from that of the present; however, sensitivity studies we have carried out under different orbital configurations (not shown), indicate that the changes discussed in this paper are robust to the change in forcing. Further justification of the choice of present-day CO_2 for the noice simulation comes from the paleo record. This indicates that during the Pliocene, about 3 MyrBP, the Greenland ice sheet was greatly reduced relative to present, and the CO_2 concentration was similar to that of the present (Raymoa et al. (1996) find a Mid-Pliocene CO_2 concentration of about 380 ppmv). This indicates that a much reduced Greenland ice sheet is not inconsistent with the climate associated with CO_2 levels similar to that of today.

In summary, there are two principal boundary condition changes applied in the noice simulation, related to the melting of Greenland: a decrease in altitude, and a decrease in albedo of the snow-free surface.

Figure 1 shows the orography in the region of Greenland in the control and noice simulations, at the resolution of the GCM. The maximum altitude is 2740 m in the control and 1020 m in the noice case. Interpolation onto the relatively coarse resolution of the GCM leads to an under-representation of the maximum bedrock height on the eastern coast of Greenland in the noice case, which is 2870 m at the 45×45 km resolution of the GREMLINS ice-sheet model. The albedo of ice-sheet in the GCM is 0.85. That of barren tundra, which replaces the Greenland ice sheet in the noice simulation, is about 0.2, but this increases if there is snow-cover. Both GCM simulations are 40 years in length. All the results presented and discussed are for the last 30 years of the simulations, unless otherwise stated. The initial 10 years allows sufficient time for an equilibrium to be attained
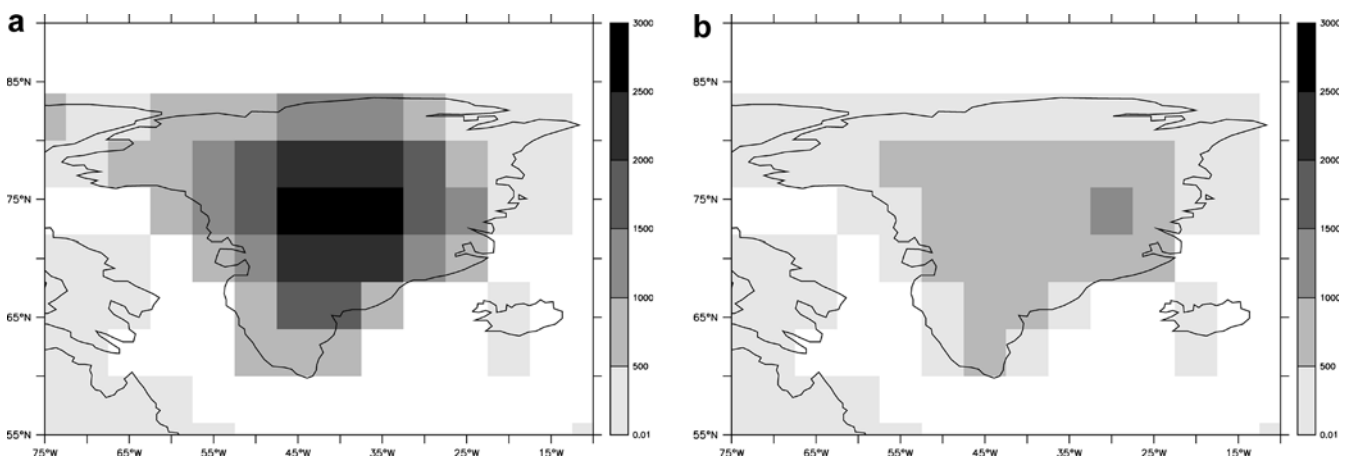

Fig. 1 a,b Orography in metres, at the resolution of the GCM, **a** in the control simulation, and **b** in the noice simulation

between the sea ice, the near-surface atmosphere, and the uppermost 100 m of the ocean.

We carry out two vegetation simulations, a control (V:control), and a no-Greenland simulation (V:noice). In the control, ORCHIDEE is driven by a present day monthly mean CRU climatology (New et al. 1999), passed through a weather generator which constructs higher frequency atmospheric forcing together with an interannual variability (J. Foley personal communication). For the V:noice simulation, we use what is known as the anomaly strategy, traditionally employed for past climate simulations, and discussed in de Noblet et al. (2000) with more references therein. The difference between the perturbed climate (noice) and the simulated present day climate (control) is added to the present day climatology, to reconstruct the forcing which is used as input to ORCHIDEE, via the weather generator. Both simulations are run at the resolution of the GCM for 500 years, starting from bare ground at all points. This allows for most vegetation types to reach their equilibrium distribution, although true equilibrium (i.e. with no further change in the area occupied by each PFT) is never reached, since the interannual variability of climate may always lead to years with, for example, very cold winters which will then kill large proportions of temperate needleleaved evergreen trees, and allow the growth of grasses and temperate deciduous trees (Lunt and de Noblet-Ducoudré 2003). A subsequent longer spin-up (20,000 years) is applied so that all carbon pools (especially soil carbon) can equilibrate, although this does not affect the PFT distribution.

For the ice sheet simulations, we also use the anomaly strategy. For the no-ice simulation (I:noice), the procedure used to force GREMLINS with GCM outputs is the same as that previously described by Charbit et al. (2002). The climatic fields driving GREMLINS are the mean annual and summer 2 m temperature, and mean annual precipitation. The temperature is expressed as a function of the temperature difference between the noice and control simulations, corrected by the difference of surface topography. The correction is made by applying a constant lapse rate (8°C per km for the annual and 6.5°C per km for the summer temperature), derived from observations (Ohmura and Reeh 1991). This difference is then added to a present day observed climatology (ERA reanalyses; Gibson et al. 1997; Kallberg 1997; this climatology is different from the one used for the GCM validation and the vegetation model anomalies, but this does not significantly affect the results). The reconstructed precipitation term, expressed as a ratio, accounts for changes in temperature between both Greenland configurations, and for changes in atmospheric circulation and hyrological cycle. The first contribution is assumed to be governed by the saturation pressure of water vapour which depends exponentially on the temperature in the atmospheric layer where precipitation is formed. With such a dependence, the temperature anomaly expressed as a difference leads to a precipitation anomaly expressed as a ratio. Because the ice-sheet model is running offline, changes in temperature due to changes in albedo are not taken into account; however, changes in temperature due to changes in altitude are included, as the forcing climate is always interpolated onto the altitude of the surface in the ice-sheet model. The I:noice simulation is for 150,000 years, which gives plenty of time for the ice sheet to respond to the climate forcing and to reach an equilibrium.

3 Evaluation of the control simulations

3.1 Climate: control

The control climate needs to be evaluated relative to observations because IPSLCM4 is a relatively new model. Here we concentrate on the SSTs, 2 m air temperature over land, 850 mbar geopotential height and temperature, precipitation, sea ice, and mid-tropospheric storm tracks. These variables are examined in detail later, in the noice case. We concentrate on the DJF season, as this is when the largest circulation changes take place when the Greenland ice sheet is removed, but also examine JJA, as summer temperatures are important for determining the development of ice-sheets, and growth of vegetation.

The global SSTs are generally simulated in good agreement with observations (not shown, AMIP; Gates 1992). In the annual mean, there is a slight warm bias of +0.05°C, equatorwards of 60°N and 60°S. The coupled model does a good job of simulating SSTs far from land, but has a warm bias off continental west coasts of up to 5°C, and a similar warm bias south of Newfoundland. The global 2 m land temperatures are also reasonably simulated with respect to observations (not shown, CRU; New et al. 1999), but there is a warm bias of +2.4°C in the annual mean. The bias is particularly strong in Northern Hemisphere high latitudes, and in siberia in DJF, is as much as +20°C. However, over Greenland itself, the temperature bias is relatively small, and over central Greenland, is less than 2°C in DJF and the annual mean. In JJA, there is a cold bias of about −3°C over central Greenland, and a warm bias of about +3°C over southeast Greenland.

Figure 2 shows the DJF air temperature at 850 mbar as simulated by the model, and the difference between this and observations (NCEP reanalysis; Kalnay et al. 1996). In the observations, extrapolation is carried out if the surface is at a higher altitude than that corresponding to 850mbar, whereas in the model there is no extrapolation, and these regions are shown as white in the plot. The zonal mean DJF temperature at this level is reasonably well simulated, but equatorwards of 75°N, there is a cold bias of about −1.4°C, and polewards of 75°N, there is a warm bias of about +0.6°C. The modelled temperatures are too warm by over 6°C to the west of Greenland, and by over 4°C over Alaska and Siberia. There is a cold bias of over 6°C east of
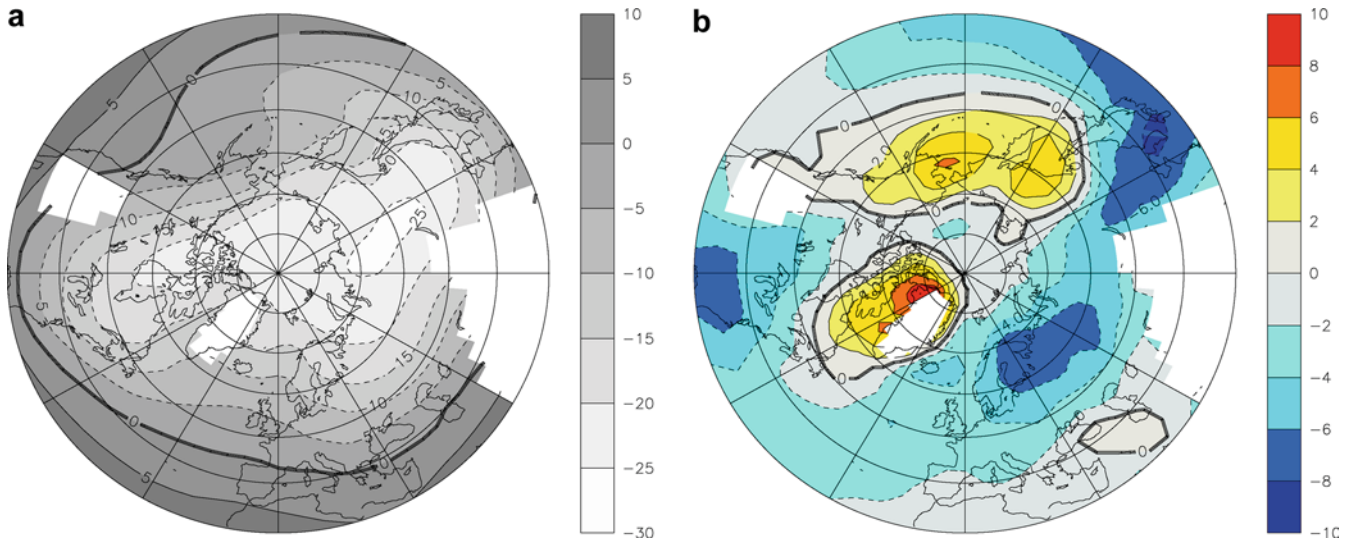
Fig. 2 a,b Temperature in °C at 850 mbar in DJF. **a** In the control simulation. **b** The control simulation minus observations (NCEP reanalysis; Kalnay et al. 1996). *White regions* are where the modelled orography is at a higher altitude than that corresponding to 850 mbar

Scandinavia and the west Pacific and east Asia. Simulated and observed temperatures are in better agreement in JJA than in DJF; warm biases of about +4°C on continental west coasts are possibly related to the too warm SSTs in the same regions. Some of the aforementioned errors in temperature are likely related to the relatively low resolution of the model. In particular, the cold bias in the mid and upper troposphere to the low vertical resolution, and regional errors in SST to the low resolution of the ocean model (OPA8.1 is usually run at 2° in longitude as opposed to the 4° used here).

Figure 3 shows the DJF geopotential height at 850 mbar as simulated by the GCM in the control simulation, and the difference between this and observations (NCEP reanalysis; Kalnay et al. 1996). The 850 mbar geopotential height in the model in the Aleutian region is too low, which could be related to cold air temperatures over the West Pacific, causing an increase in density. The low over the west Atlantic is centered too far west, resulting in near-surface Atlantic westerlies which are too weak. There is a region of high pressure in the model over the Arctic, which is more intense than in the observations. This may be contributing to the cold temperatures in northern Scandinavia, by transporting cold Siberian air westwards. In JJA (not shown), the wavenumber 2 planetary wave pattern is well simulated.
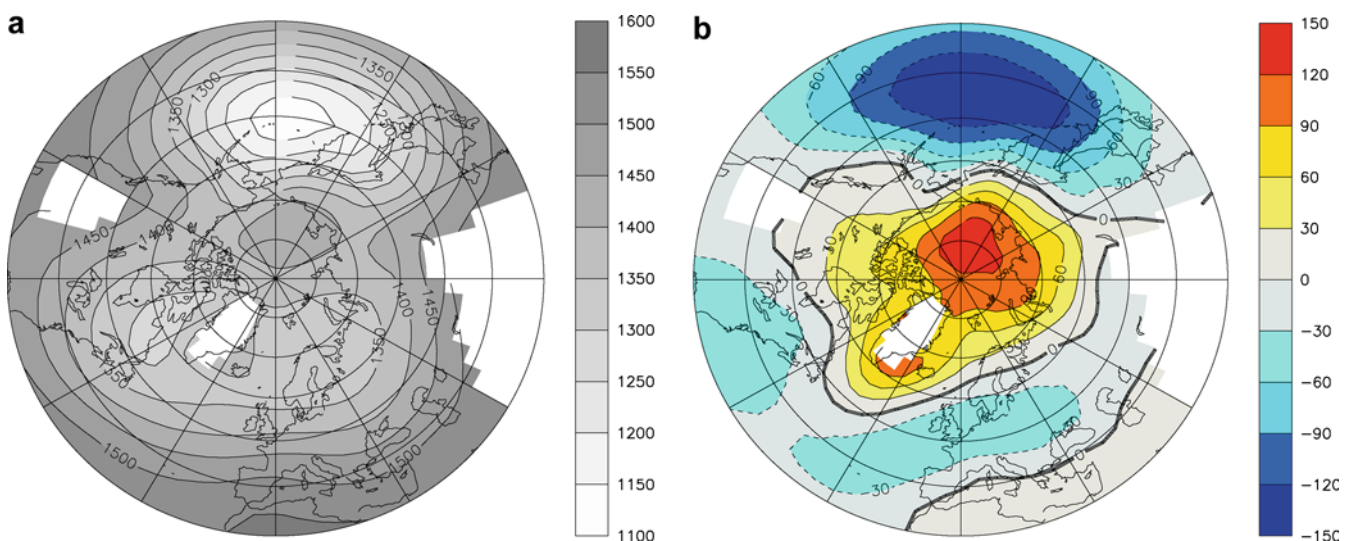

Fig. 3 a,b Geopotential height in metres at 850 mbar in DJF. **a** In the control simulation. **b** The control simulation minus observations (NCEP reanalysis; Kalnay et al. 1996). *White regions* are where the modelled orography is at a higher altitude than that corresponding to 850 mbar

In general, the winter sea-ice distribution is well simulated in the model. However, in observations (AMIP; Gates 1992), there is a tongue of sea-ice which extends from the Arctic Ocean through the Bering Straight and into the North Pacific, which is not simulated by the model. On the other hand, the sea ice reaches too far south in the model in the Barents Sea, reaching the north coast of Scandinavia. These differences are both consistent with errors in the modelled near-surface air temperatures. In JJA, the sea ice extent is also well simulated, although there is not enough sea ice to the east of Greenland, also consistent with the air temperature anomaly.

Storm-tracks are regions of high day-to-day variability, and are associated with high baroclinicity and large scale precipitation. Figure 4 shows the variability in the model and as calculated from observations (NCEP reanalysis; Kalnay et al. 1996), as the high frequency (less than 6-day) variability of the geopotential height at 500 mbar, $\bar{Z}'^{2}_{high-pass}$, which can be used as a diagnostic of storm-tracks (e.g. Hoskins and Valdes 1990). In general, the high frequency variability is underestimated in the model. There is a region of high variability over the North Atlantic in the model, with a maximum situated, in agreement with the observations, in the west Atlantic. The orientation of the Atlantic storm track is also well simulated, turning polewards along the south-east coast of Greenland. In the observations, there are significant storm tracks over the Pacific, but these are very weak in the model. Kageyama et al. (1999) have compared the storm tracks in a variety of GCMs, and the storm tracks in this model are similar to those in other GCMs of similar resolution. They find that GCMs of higher resolution (for example T42, or 3.75°×2.5°), in general simulate more intense storm tracks, in better agreement with observations. So, even though the 850 mbar geopotential height in the Aleutian region is too low, the inability of the model to correctly resolve passing weather fronts and cyclones means that the storm tracks in this region are too weak.

Northern Hemisphere winter precipitation in the model (not shown) is in general reasonably simulated compared to observations (CMAP, Xie and Arkin 1997, not shown). However, the modelled maximum in precipitation over the Pacific is situated in the east rather than in the West. This may be related to the near surface air temperatures which are too cold in the west Pacific. Over the Atlantic, the position and magnitude of the maximum of precipitation is well simulated, but it extends too far east, across the Atlantic and into the Iberian Peninsula. This is not consistent with the errors in the model storm tracks, which would lead one to expect an undersimulation of DJF precipitation. However, it may be related to the relatively cold mid-tropospheric temperatures in the model, which would lead to an increase in vertical instability in the model, and a possible increase in precipitation. The JJA precipitation is not as well simulated, there being an oversimulation of precipitation off the east coast of North America, and north of the Himalayas, of over 4 mm day^{-1}. This may be due to a warm surface temperature bias relative to observations in these regions. Over Greenland itself, in the annual mean there is too much precipitation on the west coast, by up to 4 mm day^{-1}, and in the south by about 1 mm day^{-1}. In eastern and central Greenland the precipitation is in better agreement with observations.

3.2 Vegetation: V:control and ice sheets: I:control

It is rather difficult to evaluate the present day simulated distribution of vegetation types with any actual
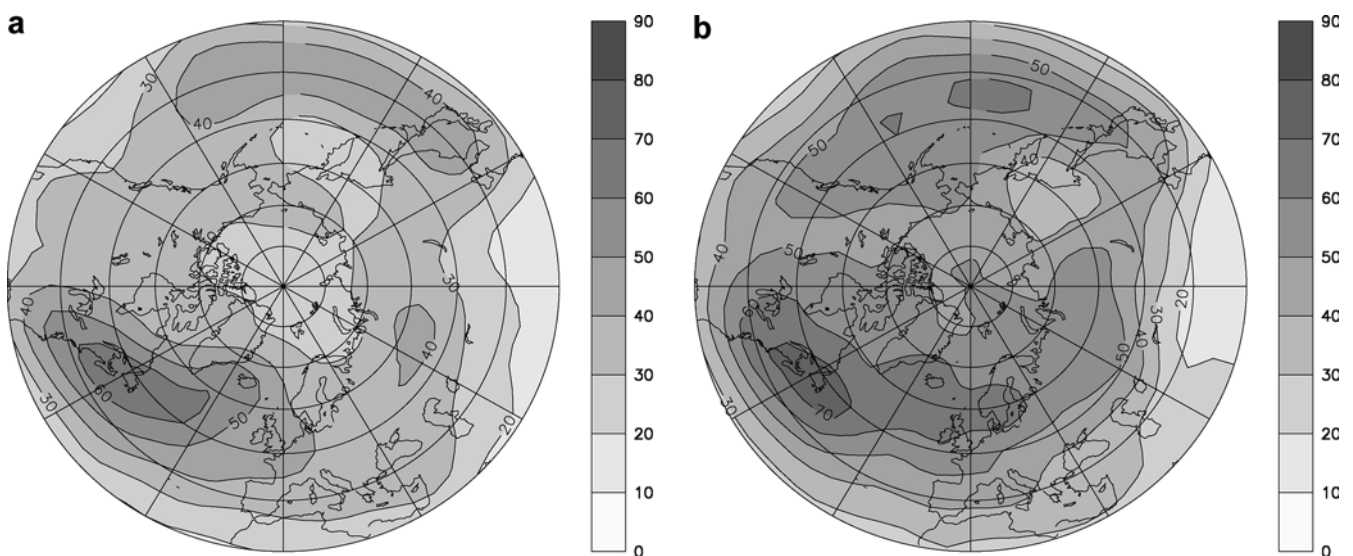

Fig. 4 a,b DJF high pass variability of 500 mbar geopotential height, $\bar{Z}'^{2}_{high-pass}$, **a** from the control simulation and **b** from observations (NCEP reanalysis; Kalnay et al. 1996)

vegetation maps, since about 40% of the landscape is covered with crops and managed prairies. ORCHIDEE is only able to simulate potential vegetation distribution, which is the vegetation which would exist if there were no human influence on the landscape. The traditional approach is to compare results with those from other dynamic global vegetation models (DGVMs). The extension of deserts and semi-arid land is well positioned and demonstrates that the temperature and rainfall thresholds used are of the correct magnitude. As in many other DGVMs, ORCHIDEE tends to grow more trees compared to grass outside of semi-arid regions, and more evergreen trees than deciduous ones. This may be partly due to the interannual variability used to drive these DGVMs at present, which could be underestimated. More discussion on the evaluation of ORCHIDEE can be found in Krinner et al. (Submitted to Global Biogeochemical Cycles).

Simulations of present-day Greenland have been performed previously by Ritz et al. (1997). The ice sheet model, GREMLINS, used in the present study has been calibrated against present day Greenland, to obtain the best fit between model results and observations.

4 The no-Greenland results

This section presents and discusses the results from the GCM, vegetation, and ice-sheet noice simulations, in which the Greenland ice sheet is removed.

4.1 Climate and circulation

The interesting changes seen in the GCM when the Greenland ice sheet is removed can be divided into two types. Firstly, there are local changes to temperature, which we will show are directly due to changes to the altitude and albedo of the Greenland surface. These surface changes do not extend far beyond Greenland itself, and are essentially independent of any circulation changes. Secondly, there are changes in the circulation throughout the troposphere, primarily as a response to the changed orography. These changes are more widespread, and are linked closely to changes in tropospheric geopotential height and temperature, and also interact with synoptic scale eddies, and surface temperature outside of Greenland, primarily by interaction with the sea-ice. We also consider precipitation changes which are important when we look at changes to vegetation on Greenland, and the growth of the Greenland ice sheet.

We start by looking at the surface temperature changes locally over Greenland in DJF and JJA seasons. We go on to look at atmospheric and oceanic changes, and link together changes in geopotential, temperature, sea-ice, and heat transport by both the time mean circulation and eddies. In the atmospheric case, the changes are most interesting in DJF when the northern hemisphere atmosphere is more unstable. In this section, all changes have been tested with Student T-test, and we only discuss those which are more than 90% significant.

4.1.1 Local surface temperature changes

Figure 5 shows the change in 2 m temperature, noice-control, for DJF and JJA. In both seasons, the largest change in surface temperature is over Greenland itself. In DJF, the maximum mid-Greenland temperature increase is 14°C; in JJA, it is 21°C. Averaged over the Greenland region (defined as being 60°N to 85°N, and 20°W to 60°W, the temperature increase is 4.0°C in DJF, and 8.5°C in JJA. Also present in DJF is a region of decrease of surface temperature, centred over the
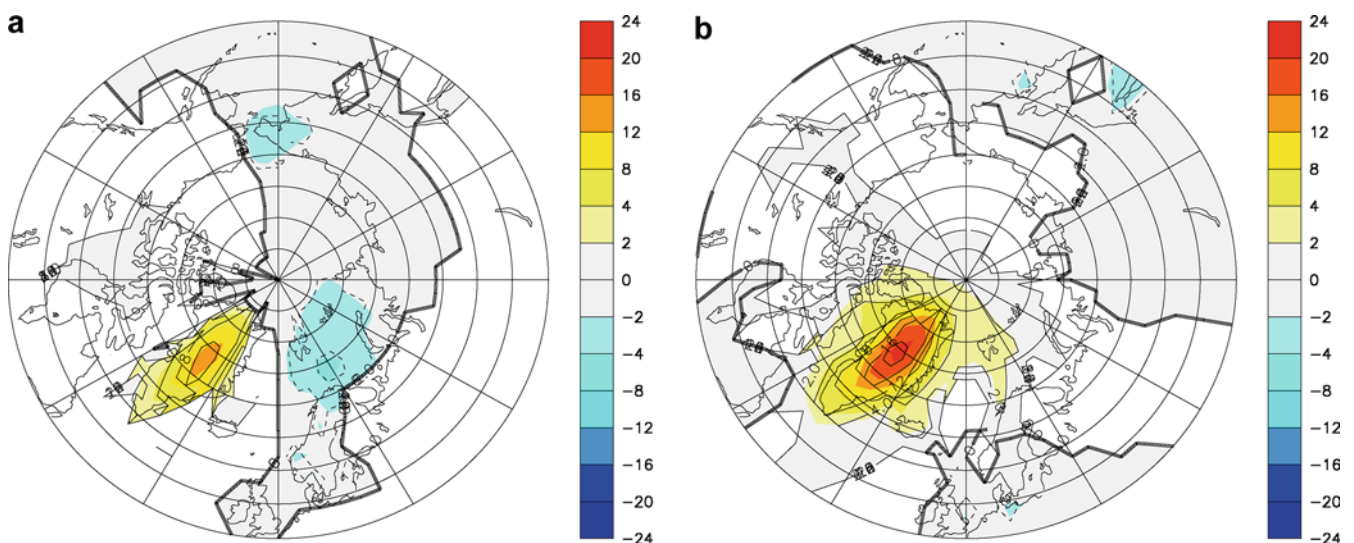

Fig. 5a,b Two meter temperature change in °C, noice-control, **a** in DJF and **b** in JJA. Note the non-linear scale. *White regions* are those where the statistical significance is less than 90%, as given by a Student *T*-test

Barents Sea, in the Arctic Ocean north of Scandinavia. There is a similar, less intense decrease, centered on the Bering Sea. It is clear that the principal effect of removing the Greenland ice-sheet is relatively localised.

To allow a greater understanding of all the changes seen in the noice simulation, we have also carried out a further GCM simulation (lowice) in which we lower the orography over Greenland to the bedrock level, as in the noice simulation, but leave the surface characteristics (including albedo) as those of the ice sheet. The lowice simulation is similar to the nogreen simulation of Petersen et al. (2004), except where we set the orography to the bedrock, they set the orography to sea level. In simulation lowice, the DJF temperature change over Greenland compared to the control is +4.1°C. This is very similar to the +4.0°C in the noice case. This similarity is explained by the fact that in DJF, at these high latitudes, the daily mean insolation is very low (only 0.2 Wm^{-2} of solar radiation is absorbed at the Greenland surface in DJF), and so the DJF temperature increase in the noice case is not related to any change in albedo, which produces a temperature change which depends on the intensity of the insolation. Furthermore, in DJF it is cold enough in noice so that all the precipitation falls as snow, resulting in a DJF albedo which is in fact very similar to that in control. The magnitude of the DJF temperature change over Greenland, in both the noice and lowice simulations, is also consistent with a simple lapse-rate calculation. The decrease in altitude alone would be expected to cause a surface temperature change of approximately $-\Gamma \Delta z$, where Γ is the lapse rate, and Δz is the change in altitude. Taking Γ as the mid-tropospheric DJF value from the simulation, this gives a Greenland average temperature change of about 4°C. This suggests that circulation changes are not important in determining the temperature change locally over Greenland in DJF.

In JJA, the temperature change due to the change in altitude alone is given by the difference in 2 m temperature over Greenland between lowice and control, of 3.3°C. This is less than the DJF value of 4.1°C because in DJF there is a temperature inversion just above the surface in the control experiment, which is not present in lowice. This means that the control surface temperature is relatively cold compared to the lowice surface temperature, and means that the lowice–control difference is greater in DJF than in JJA, when neither simulation has an inversion. In JJA, the surface of Greenland absorbs significantly more downwelling short-wave radiation in the noice case (150 W m^{-2}) than in the control (50 W m^{-2}). This is due to the lower albedo in noice, and results in warmer surface Greenland temperatures in noice. Neglecting possible contributions from changes in circulation, it can therefore be said that in JJA, the total temperature change of 8.5°C is made up of an albedo effect of 5.2°C, and an altitude effect 3.3°C.

The 2 m air temperature change is more localised in DJF than in JJA, possibly due to the fact that the albedo change in JJA actually results in an input of heat into the atmosphere, which can then be advected away, whereas the change in 2 m temperature in DJF is principally a result of the altitude at which the temperature is measured.

4.1.2 Tropospheric temperature and circulation changes

DJF Figure 6 shows the DJF geopotential height change at 500 mbar, noice–control. This varies little throughout the troposphere, due to the barotropic nature of the response. We show 500 mbar rather than sea level pressure because this avoids the need to extrapolate over regions of orography, and in particular over Greenland itself. There is a decrease in geopotential height over southern, central and western Greenland, which extends and deepens over the North Atlantic. This decrease in geopotential height over the decreased orography is consistent both with previous GCM work (Toniazzo et al. 2004), and with theory (Hoskins and Karoly 1981). There is an increase in geopotential to the east of Greenland, which extends and becomes more intense over Scandinavia and into central Eurasia. There is also an increase in geopotential to the west of Greenland, which is seen also by Petersen et al. (2004), who attribute it to cold air in the control simulation over northern Canada, which can not be advected away by passing cyclones due to the blocking effect of the Greenland orography. Also, the results can be interpreted as the removal of the Greenland ice sheet decreasing the amplitude of the planetary waves, resulting in a change in geopotential which mirrors the absolute geopotential, which has a wavenumber two characteristic at high latitudes. There are also more remote changes; overall, the response appears to be mainly
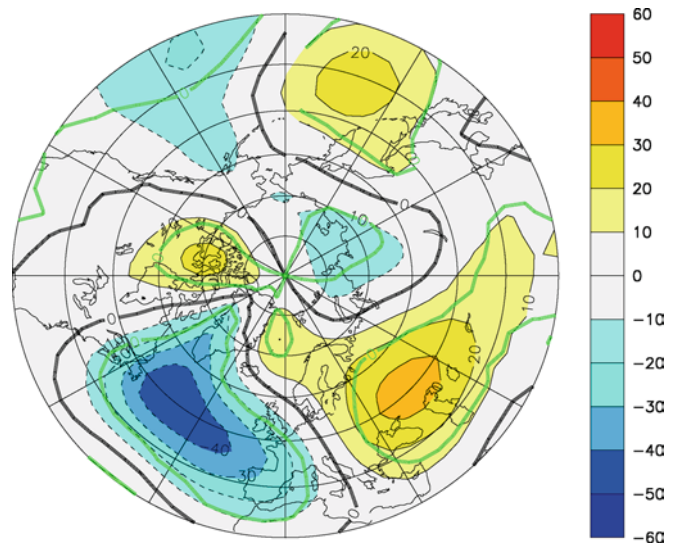

Fig. 6 DJF geopotential height anomaly change, minus zonal mean, in metres, noice-control, at 500 mbar. The green line encloses those regions where the statistical significance is greater than 90%, as given by a Student *T*-test
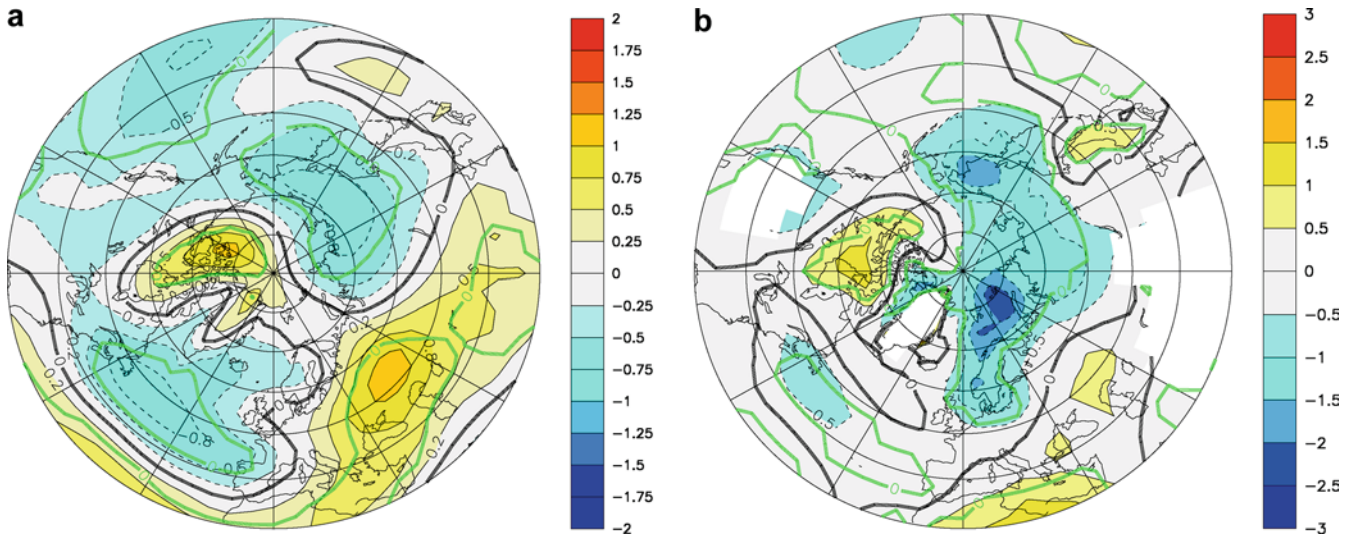
Fig. 7a,b DJF temperature change in °C, noice-control, **a** at 500 mbar and **b** at 850 mbar. Note the difference in scale between the two plots. White regions in **b** are where the modelled orography in the control simulation is at a higher altitude than that corresponding to 850 mbar. The *green lines* enclose those regions where the statistical significance is greater than 90%, as given by a Student *T*-test

wavenumber three in mid latitudes and wavenumber two at polar latitudes.

Figure 7a shows the difference in DJF air temperature, noice–control, also at 500 mbar. This is very similar in form to, and consistent with, the geopotential change. The exception is over Greenland itself, where there is a decrease in geopotential, but an increase in temperature. This is because 500 mbar is close to the surface in the control simulation, where the air temperatures are reduced by the relatively cold ice-sheet surface. Further from the surface, there is actually very little difference in temperature between the two simulations over Greenland itself. Figure 7b is the same but at 850mbar. Here there are also some correlations between the geopotential and temperature change. However, it can be seen that there is significant interaction with the surface. The regions where the noice simulation is cooler than the control at 850 mbar, in particular over the Barents and Bering Seas where there is a cooling of 2.0°C and 1.5°C respectively, are also cooler at 2 m (see Fig. 5a). This can partly be understood in terms of the near surface atmospheric circulation change. Associated with the tongue of increased geopotential which extends from Eurasia, up to the east of Greenland, there is a significant change in near-surface meridional wind speed over the Barents Sea. The change in wind velocity at 500 mbar over Greenland and the Barents Sea, is shown in Fig. 8. The figure shows that in the noice simulation, there is increased meridional transport from the pole, southwards over the Barents Sea, resulting in colder air near the surface (both simulations have a southwards wind component in this region, but in noice it is stronger). This colder air results in an increase in sea-ice coverage in the Barents Sea in the noice simulation relative to the control, which is also shown in Fig. 8. The change from an ocean surface to a sea-ice surface allows

the model to further decrease the surface temperature in response to the atmospheric forcing. The colder air temperatures, linked to the surface type change and the atmospheric circulation change, propagate upwards in the lower troposphere, but are no longer evident at 500 mbar. A similar mechanism can be used to explain the low temperatures in the Bering Sea in the noice simulation, which are also associated with an increase in sea-ice cover, and a change in meridional transport, linked with the low-high pressure dipole response over the Pacific.

JJA In JJA, the temperature change throughout the lower and middle troposphere is dominated by the warming over and around Greenland. The increase of sea-ice in the Barents Sea seen in DJF is also present in JJA, and results in cooler surface temperatures in the Barents Sea, but it is not sufficient to cause a decrease in
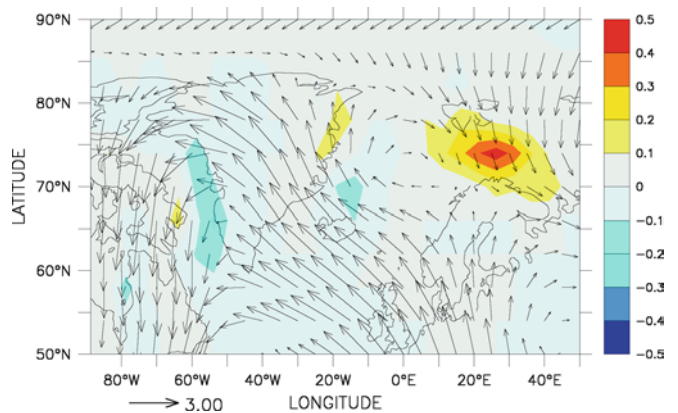

Fig. 8 Vectors show the change in wind velocity, noice–control, at 500 mbar in DJF. *Colour shading* shows the fractional change in DJF sea-ice cover

the near-surface air temperature. In JJA, the geopotential response to the local heating anomaly over Greenland is also largely barotropic, and is a ridge to the northeast of Greenland, and an associated trough to the south, centred over southern Scandinavia. The strong surface summer warming has consequences for the development of both vegetation on Greenland, and the regrowth of the ice sheet, as we show in Sects. 5.2 and 5.3.

4.1.3 Oceanic, precipitation and storm-track changes

The SST changes are similar to the 2 m air temperature changes, shown in Fig. 5, and are relatively small, except for warmings just off the southern tip of Greenland, of about 1°C in DJF and about 2°C in JJA, and where there are changes to the sea-ice cover. In the deep ocean, there are no significant changes to the circulation or temperature. Figure 9 shows the change in DJF precipitation, noice–control. The increase in precipitation off the west coast of the Iberian Peninsula is due primarily to changes in convective precipitation, whereas other changes are due to the large-scale precipitation. There is an intense and localised decrease in precipitation in west Greenland in the noice simulation, and a corresponding increase in precipitation in east Greenland. In both the control and noice simulations, the mid-tropospheric air flow is from Newfoundland, north and east over the Greenland plateau, and then eastwards (in observations (NCEP reanalysis; Kalnay et al. 1996), the flow is slightly more zonal, and the air masses reaching the west coast of Greenland at 500 mbar arrive from further north). The precipitation occurs primarily in the control when the air mass encounters the high Green-

land orography. In the reduced-orography noice simulation, the change in altitude is not so sudden, and so the precipitation is less intense, but over a larger area. Toniazzo et al. (2004) also find increased precipitation in eastern Greenland, but both they and Petersen et al. (2004) also find a large decrease at the southern tip of Greenland, which we do not see. This may be due to the higher horizontal resolution of their models, which better represent the orography. In our noice simulation, there is also a decrease in large scale precipitation over the West Atlantic, off the coast of Newfoundland, and a corresponding increase to the south. This change can be understood in terms of changes to the storm tracks; Fig. 10 shows the change in the variance of the 500 mbar geopotential height, as in Sect. 1, noice–control. The main change in the storm track is that in the noice simulation it does not veer as strongly northwards up the south-east coast Greenland as in the control. This is apparent in the dipole structure of the change, with a minimum south-east of Greenland, and a maximum further south. In the noice simulation, the Atlantic storm track is also weakened further west, off the coast of Newfoundland, north of 50°N. The reason for this weakening may be the decrease in the meridional temperature gradient at 500 mbar over the Atlantic, north of 50°N (see Fig. 7), which would lead to a decrease in vertical wind shear, and baroclinicity. This decrease is also consistent with the decrease in large scale precipitation off the coast of Newfoundland. Similarly, in the same region but southwards of 50°N, the Atlantic storm track is slightly intensified. In this region, there is an increase in the meridional temperature gradient at 500 mbar. This is also consistent with the increase in large scale precipitation in the same region. The decrease in storminess over the North Atlantic in the noice sim-
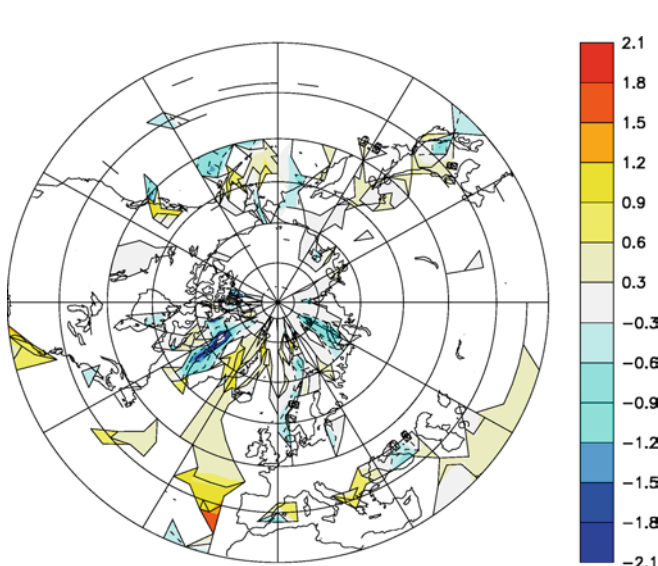

Fig. 9 Change in DJF precipitation, in millimeter per day, noice–control, zero contour suppressed. *White regions* are those where the statistical significance is less than 90%, as given by a Student *T*-test
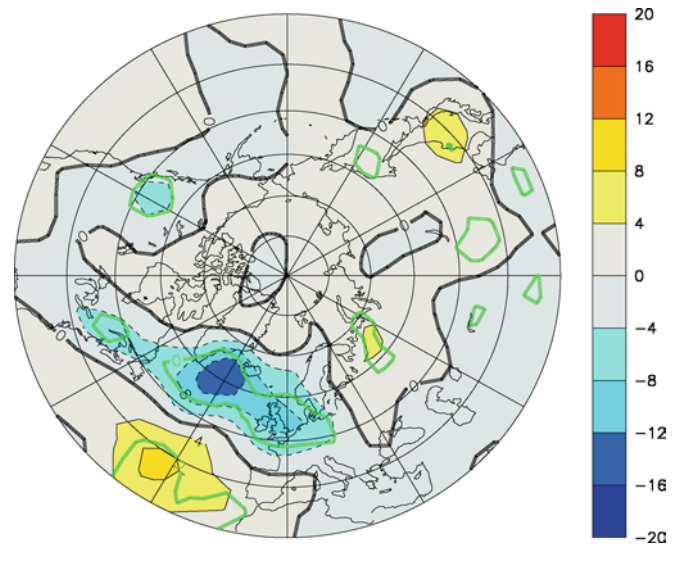
Fig. 10 Change in DJF high pass variability of 500 mbar geopotential height, $\Delta \bar{Z}'^2_{high-pass}$, noice–control. The green line encloses those regions where the statistical significance is greater than 90%, as given by a Student *T*-test

ulation, and the associated decrease in polewards heat transport, may also be a contributing factor to the decrease in the lower troposphere air temperature over the Barents Sea, which is the driving mechanism for the increase in sea-ice.

4.2 Vegetation

In the V:control simulation, Greenland is covered with an ice-sheet (Fig. 11a), while the boundary condition used to run the noice GCM simulation prescribed a tundra vegetation consisting of about 35% grasses, very few trees, and mostly bare ground (Fig. 11b). The resulting climate change induced by the prescribed changes over Greenland is sufficient to not only maintain vegetation over most of Greenland (Fig. 11c), but also to allow for the growth of trees in south-western Greenland and along the eastern coast. Grasslands dominate most of the interior continent while totally bare ground is found only at the extreme North. This distribution of vegetation is most closely controlled by temperature. At the extreme North, the cumulated degree day temperature (above 0°C) does not exceed 150°C, the minimum required for any kind of plant to grow. Further south, the growth of trees is not only conditioned by available moisture but also by winter temperatures. Below certain critical thresholds trees will not grow, but where these thresholds are exceeded, due

to the orography-induced warming, trees dominate. The annual net primary productivity of trees simulated in these areas range between 350 and 500 g cm^{-2}, which is well above the minimum required of 140 g cm^{-2} discussed by Kaplan et al. (2003). Outside of Greenland, the only significant change in vegetation distribution is a small northward expansion of trees, in North America, east and west of the Hudson Bay. All increases in tree area have about the same partitioning between evergreen and deciduous trees, with no specific predominance. This simulation shows that in fact, where we put tundra over Greenland into the noice-GCM simulation, a mixture of trees and grass would have been more appropriate. This has some implications for the ice sheet simulations which follow.

4.3 The regrowth of the Greenland ice sheet

Figure 12a shows the thickness of the ice sheet at the end of the I:noice simulation, when equilibrium has been reached. It is clear that a substantial ice sheet is simulated in eastern and central Greenland. Using GCMs, previous workers (Toniazzo et al. 2004; Crowley and Baum 1995) have used the evolution of surface snow mass as an indicator of ice-sheet growth, and concluded that an ice-sheet would not be able to develop once it had melted. If the snow cover does not melt over summer, then the snow mass in a GCM will increase year by

Fig. 11a–c The dominant vegetation type in each gridbox. **a** Present day potential vegetation as simulated by ORCHIDEE (V:control). **b** Vegetation cover used in the GCM simulation noice. **c** Vegetation cover with a melted Greenland ice sheet, simulated by ORCHIDEE (V:noice), forced by the noice climate
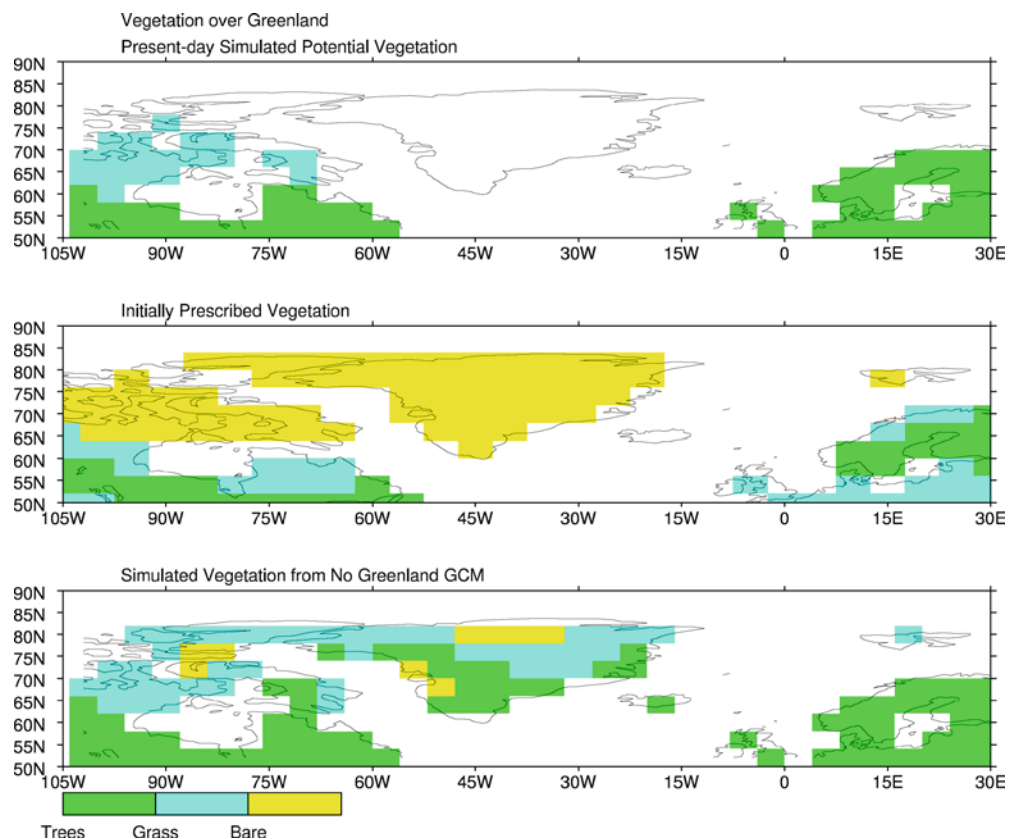
year. Figure 12b shows the snow cover in the GCM-noice simulation, from the last year of the simulation. At each gridbox, the snow-cover plotted is that of the month with the least snow cover. Non-zero values are therefore an indication of possible ice-sheet growth. It is clear that the two diagnostics are incompatible. The GCM-noice snow cover indicates ice-sheet development only in Ellesmere Island, northwest of Greenland. This is consistent with the ground temperature in the noice-GCM simulation, as this is the only northern hemisphere land mass which has permanently sub-zero temperatures. The main cause of the difference between the two diagnostics is the high resolution of the ice sheet model, although the climate is also different, whereas the GCM sees the absolute temperature and precipitation, the ice sheet model sees the temperature and precipitation calculated by the anomaly method. The high resolution means that the ice sheet model sees regions of very high altitude, which are not represented by the GCM. Glaciers form on most of the high altitude regions in eastern Greenland, in particular those around 70°N. The glaciers can then flow into regions which are otherwise at relatively low altitude. This allows the gradual build up of an extensive ice sheet, even covering regions of relatively low bedrock. It is clear that the summer soil temperatures over central Greenland in the GCM, which are up to about 8°C, are not so warm as to prevent the growth of the ice sheet. The growth of the ice sheet in eastern Greenland is also being aided by the increase in (solid) precipitation in this region, shown in Fig. 9 for DJF, but actually occurring throughout the year. In eastern Greenland, where the ice sheet is being initiated, the precipitation in the control simulation is well simulated compared to observations. However, in the west this is not the case, and it is possible that a better simulation of precipitation in the control simulation would result in a smaller increase in precipitation in the noice simulation, and would make the Greenland ice sheet grow more slowly, or reach a smaller equilibrium size,

due to the drier climate over Greenland. However, we believe that this would not change our conclusion that the ice sheet would at least start to regrow. This drier climate could result from a better simulation of the mid-tropospheric flow over Greenland, with the air masses which arrive at Greenland's west coast originating from further north.

The implication of this ice sheet simulation is that if the Greenland ice sheet were to completely melt, due to increased greenhouse gas concentrations, which were then reduced back to present day levels, then our work suggests that the ice sheet would recover. It is very likely that if a further iteration were carried out, and the GCM run with the ice sheet in Fig. 12a, then the resulting local summer climate would be cooler than the noice climate, due to the albedo effect, and would be able to support a larger ice sheet. This implies that given present day greenhouse gas concentrations, the Greenland ice sheet is not bistable (i.e. it can not exist in a stable state both with and without an ice sheet), but will grow an ice sheet if one is not present, due to the high altitudes in eastern Greenland, which act as a trigger for ice sheet growth. It is possible that with higher greenhouse gas concentrations, the ice sheet may be bistable, but it would require further sets of simulations to investigate this. One caveat to this is that our vegetation simulation indicates that a large fraction of Greenland is likely to become covered in trees if the ice sheet were to melt. This would raise the summer albedo, and possibly result in a smaller equilibrium ice-sheet.

5 Discussion

How does this work compare to previous studies? The most relevant study is that of Toniazzo et al. (2004), with which some comparisons have already been drawn. They carry out similar GCM simulations to ours, but with the HadCM3 fully coupled atmosphere-ocean model
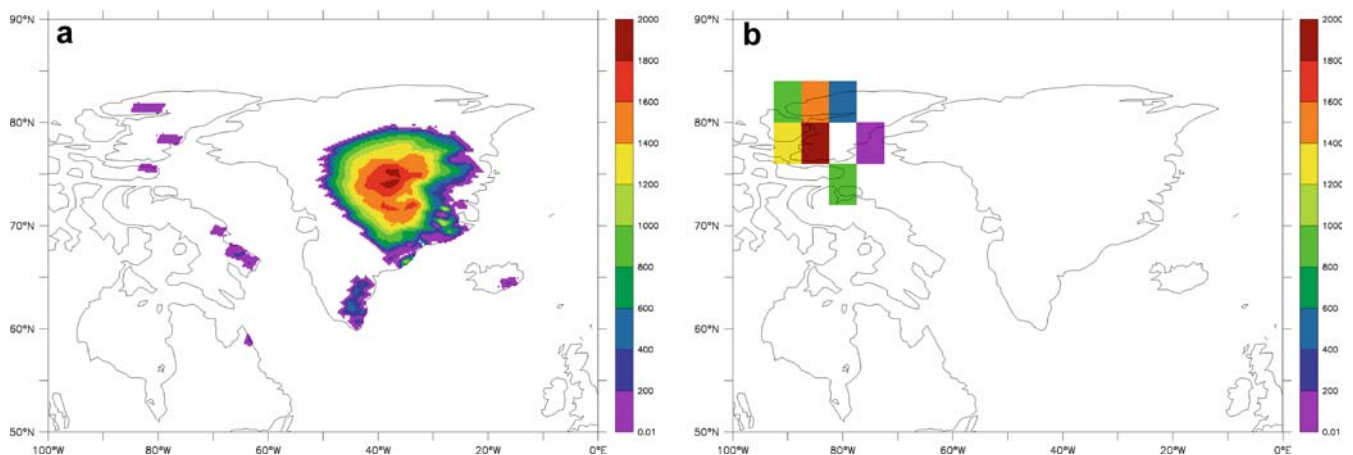

Fig. 12 a Ice sheet thickness at the end of the I:noice simulation, i.e. as predicted by GREMLINS forced by the noice climate. **b** Surface snow mass (kg m^{-2}) of the least snowy month, in the last year of the GCM simulation noice

(Gordon et al. 2000; Pope et al. 2000). They simulate an annual mean temperature increase over Greenland of $+6.7°C$, compared to our $+5.7°C$, and have similar changes to the radiation budget over Greenland. In agreement with us, they simulate a cooler winter Barents Sea, and attribute this to changes in the storm tracks, but they do not see an associated substantial increase in sea ice, and do not link this to changes in the time mean circulation. They have substantial sea-ice increases to the west and south of Greenland, and associated temperature decreases, which are not present in our simulation. It therefore seems that in terms of temperature, the changes over Greenland itself are a robust feature, independent of the climate model (assuming our and their assumption of an unchanged thermohaline circulation is correct), whereas more remote changes are not. An exception is the cooling over the Barents Sea, which is common to both models. The decrease in strength of the North Atlantic storm tracks is also a robust feature between the two models. A further comparison can be made with the transient simulations of Loutre and Kageyama (2003), described in Sect. 2. After Greenland melted, northern hemisphere glaciation did not reach present levels during their entire 200,000 year simulation, and the Greenland ice sheet did not start regrowing until long after the return to present day CO_2 levels, about 60,000 years in the future. However, their transient simulations included variations in solar forcing which are not included in our equilibrium simulation; when CO_2 levels fall back to present day values in their simulations the solar forcing in northern hemisphere summer is high, which hinders the reglaciation. Furthermore, whereas the GCM fields used to force the ice-sheet model in our simulation are anomalies from the present day control, Loutre and Kageyama (2003) use absolute forcings from their climate model.

One weakness of the GCM approach is that it is not very efficient to carry out transient simulations of the complete melting of Greenland, due to the long time-scales involved. This makes it difficult to investigate the effects of the expected flux of fresh water into the ocean, resulting from the melting of Greenland. It is possible that such a flux would have significant implications for the thermohaline circulation, and therefore SSTs and the whole climate system. An appropriate tool for investigating this problem is the EMIC, CLIMBER (Ganopolski et al. 1998). Ganopolski and Rahmstorf (2001) have used this model to carry out experiments in which various freshwater fluxes are applied to the North Atlantic. They find a freshwater flux threshold of about 0.07 Sv for a collapse of the thermohaline circulation. This corresponds to a constant melting over about 1,400 years (assuming a Greenland ice-sheet volume of 3×10^6 km³). This is significantly shorter than the 4,700 years predicted by Loutre and Kageyama (2003) for a complete melting of the Greenland ice sheet, and this gives some confidence that we can safely neglect the freshwater flux. In fact, the 0.07 Sv threshold in CLIMBER is considered a low estimate, and the

HadCM3 (Gordon et al. 2000; Pope et al. 2000) thermohaline circulation weakened but did not collapse with 1.0 Sv (J. Gregory, University of Reading, UK, personal communication). Recently, Fichefet et al (2003) have carried out a transient GCM/ice sheet model simulation of the melting of the Greenland ice sheet, over the timescale of the next century. In their work, the North Atlantic overturning circulation was substantially reduced about 80 years from the present, following continuous freshwater input of about 0.015 Sv, resulting in cooler temperatures in the North Atlantic by about 2°C compared to present. These cooler temperatures would possibly slow the melting of the ice sheet, indicating that the Greenland ice sheet is perhaps more stable than previous simulations would suggest. Unfortunately, they did not extend their simulations beyond the end of the twenty-first century, and so could not indicate whether the thermohaline circulation would recover, or over what timescale. Furthermore, their freshwater flux is relatively very weak, and it is perhaps surprising that such a large response was observed. Experiments we have carried out with the CLIMBER model (not shown), in which an artificially large fresh water flux, corresponding to a complete melting of the ice sheet in 50 years, was added to the North Atlantic at the same time as the orography and ice sheet over Greenland was reduced, showed a recovery in the thermohaline circulation after the timescale of a few centuries, and the system equilibrated to the same state as that with no freshwater input. However, all these results could well be model dependent, and more work is required with more complex models. In conclusion, we can say that by neglecting the freshwater in the GCM-noice simulation, and by using a bedrock appropriate for about 4,000 years in the future, we are consistently simulating the earth system after a 'slow' melt of the Greenland ice-sheet in which the thermohaline circulation did not collapse, or equally well, simulating the earth system after a 'fast' melt in which the thermohaline circulation did collapse, but subsequently recovered and returned to the initial state. The ocean model we have used, with the damped ocean temperatures and salinities, is not an appropriate tool to investigate this further. In the future, transient experiments with the fully coupled version of IPSLCM4 (i.e. without damping), in which freshwater fluxes are added in appropriate regions for a Greenland melt, could be carried out.

6 Conclusions

We have evaluated the IPSLCM4 GCM, and shown it to simulate reasonably well certain aspects of the current climate. We have used this GCM to carry out two principal simulations: a present day control, and a simulation in which the Greenland ice sheet is removed. We have shown, using a further simulation in which the altitude is reduced over Greenland but the surface type kept as ice-sheet, that locally over Greenland, the DJF

surface temperature increase is due solely to the decreased altitude. This is due to the very low insolation at high northern hemisphere latitudes in DJF. We have shown that 40% of the JJA temperature increase is due to the decreased altitude and 60% due to the change in surface type, specifically albedo. Outside of Greenland, we have related the DJF temperature decrease over the Barents Sea to interactions with the sea-ice cover, and changes in the time mean atmospheric circulation due to the decreased Greenland orography, and to decreased poleward heat transport due to a decrease in storm activity due to a decrease in the meridional temperature gradient over the North Atlantic. We attribute the increased East Greenland precipitation, and decreased West Greenland precipitation, to the decrease in Greenland orography.

The GCM-simulated climates are used to force the ORCHIDEE vegetation model offline. This shows that the absence of a Greenland ice sheet allows the growth of trees in southern Greenland, and grass over most of the rest of Greenland. The type of dominant vegetation is controlled most closely in these regions by the temperature of the coldest month. The GCM climates are also used to force the GREMLINS ice-sheet model. This indicates that following a complete melting, the Greenland ice-sheet could regrow, provided that the greenhouse gas concentrations returned to their present day values. This is in contradiction with previous workers who suggested that the Greenland ice sheet may be bistable under present day forcing (Crowley and Baum 1995; Toniazzo et al. 2004). It is possible that with future stable elevated greenhouse gas concentrations, perhaps due to vegetation/climate feedbacks, the ice sheet would not regrow, but this remains to be investigated. A possible mechanism for the regrowth is a 'seeding' of the ice-sheet in high altitudes in eastern Greenland, which subsequently flows into the lower altitude regions of central Greenland. We have shown the build-up of snow-cover in the GCM itself to be a poor diagnostic of ice-sheet growth, due primarily to the low resolution.

In future, it would be informative to carry out more in-depth studies into the mechanisms of change. An example is the lowice simulation described earlier, which shows the relative importance of the albedo and altitude change. Future studies should involve cutting feedback loops, for example by keeping the SSTs and sea-ice constant, to assess their importance. Concerning the GCM itself, the most recent version of IPSLCM4, not used for this work, has an improved present day climatology, related in part to the inclusion of Emanuel (1991) convection scheme, in the place of that of Tiedtke (1989), and should be used for future studies. In addition, more work should be carried out to assess the effects of using the damped ocean, by carrying out both fully coupled and damped simulations, under a variety of climate forcings. Another interesting study would be to impose relatively cool SSTs in the North Atlantic to simulate a shutdown of the thermohaline circulation.

Unfortunately, due to CPU constraints, this was not possible in the framework of this study.

Future work should also investigate the transient system in more detail. This could include asynchronous coupling of the three components of the earth system investigated here: atmosphere/ocean, vegetation, and ice-sheets. It may be, for example, that the presence of trees in southern Greenland, which our vegetation simulations show is likely, would result in a warmer Greenland climate due to decreased albedo which would inhibit ice-sheet growth. A fully transient experiment should be carried out with an EMIC, capable of fully coupling the components of the earth system. An example is GENIE (Marsh et al. 2003), a model currently under development, which unlike traditional EMICS, will be capable of a physical representation of short-timescale atmospheric processes such as mid-latitude storms, as well as having three dimensional ocean and ice-sheet components.

References

Blanke B, Delecluse P (1993) Variability of the tropical atlantic ocean simulated by a general circulation model with two mixed layer physics. J Phys Oceanogr 23:1363–1388

Charbit S, Ritz C, Ramstein G (2002) Simulations of northern hemisphere ice-sheet retreat: sensitivity to physical mechanisms involved during the last deglaciation. Quaternary Sci Rev 21:243–265

Crowley TJ, Baum SK (1995) Is the Greenland ice sheet bistable. Paleoceanography 10:357–363

de Noblet N, Claussen M, Prentice CI (2000) Mid-Holocene greening of the Sahara: first results of the GAIM 6,000 year BP experiment with two asynchronously coupled atmosphere/biome models. Clim Dyn 16:643–659

de Rosnay P, Polcher J (1998) Modelling root water uptake in a complex land surface scheme coupled to a GCM. Hydrol Earth Syst Sci 2:239–255

Ducoudré NI, Laval K, Perrier A (1993) SECHIBA, a new set of parameterizations of the hydrologic exchanges at the land-atmosphere interface within the LMD atmospheric general circulation model. J Clim 6:248–273

Emanuel K (1991) A scheme for representing cumlus convection in larg scale models. J Atmos Sci 48:2313–2335

Felzer B, Oblesby RJ, Webb T, Hyman DE (1996) Sensitivity of a general circulation model to changes in northern hemisphere ice sheets. J Geophys Res 101:19077–19092

Fichefet T, Morales Maqueda MA (1999) Modelling the influence of snow accumulation and snow-ice formation on the seasonal cycle of the Antarctic sea-ice cover. Clim Dyn 15:251–268

Fouquart Y, Bonnel B (1980) Computation of solar heating of the Earth's atmosphere: a new parameterisdation. Beitr Phys Atmos 53:35–62

Ganopolski A, Rahmstorf S (2001) Rapid changes of glacial climate simulated in a coupled model. Nature 409:153–158

Ganopolski A, Rahmstorf S, Petoukhov V, Claussen M (1998) Simulation of modern and glacial climates with a coupled global model of intermediate complexity. Nature 391:311–356

Gates WL (1992) AMIP: the atmospheric model intercomparison project. Bull Am Meteorol Soc 73:1962–1970

Gent PR, McWilliams JC (1990) Isopycnal mixing in ocean circulation models. J Phys Oceanogr 20:150–155

Gibson JK, Kallberg P, Uppala S, Herandez A, Nomura A, Serrano E (1997) ERA description, ECMWF Re-analysis project series 1, Reading, UK

Hoskins BJ, Karoly DJ (1981) The steady linear response of a spherical atmosphere to thermal and orographic forcing. J Atmos Sci 38:1179–1196

Hoskins BJ, Valdes PJ (1990) On the existence of storm tracks. J Atmos Sci 47:1854–1864

IPCC (1995) Climate change 1995: the science of climate change. In: Houghton JT, Meira Filho LG, Callander BA, Harris H, Kattenberg A, Maskell K (eds) Contribution of working group i to the second assessment report of the intergovernmental panel on climate change, Cambridge University Press, Cambridge, UK, pp 572

IPCC (2001) Climate change 2001: the scientific basis. In: Houghton JT, Ding Y, Griggs DJ, Noguer M, van der Linden PJ, Dai X, Maskell K, Johnson CA (eds) Contribution of working group I to the third assessment report of the intergovernmental panel on climate change. Cambridge University Press, Cambridge, NY, USA, pp 881

Kaplan JO, Bigelow NH, Prentice IC, Harrison SP, Bartlein PJ, Christensen TR, Cramer W, Matveyeva NV, McGuire AD, Murray DF, Razzhivin VY, Smith B, Walker DA, Anderson PM, Andreev AA, Brubaker LB, Edwards ME, Lozhkin AV (2003) Climate change and arctic ecosystems II: modeling, paleodata-model comparisons, and future projections. J Geophys Res 108:8171. Doi 10.1029/2002JD002559

Kageyama M, Valdes PJ, Ramstein G, Hewitt C, Wyputta U (1999) Northern hemisphere storm tracks in present day and last glacial maximum climate simulations: a comparison of the european PMIP models. J Clim 12:742–760

Kallberg P (1997) Aspects of the re-analyzed climate. In: ECMWF Re-analysis Project Series 2, Reading, UK

Kalnay E, Kanamitsu M, Kistler R, Collins W, Deaven D, Gandin L, Iredell M, Saha S, White G, Woolen J, Zhu Y, Chelliah M, Ebisuzaki W, Higgins W, Janowiak J, Mo KC, Ropelewski C, Wang J, Leetma A, Reynolds R, Jenne R, Joseph D (1996) The NCEP/NCAR 40-year reanalysis project. Bullet Amer Meteorol Soc 77:437–471

Krinner G, Viovy N, de Noblet-Ducoudré N, Ogée J, Friedlingstein P, Ciais P, Sitch S, Polcher J, Prentice IC A dynamical global vegetation model for studies of the coupled atmosphere-biosphere system (Submitted to Global Biogeochemical Cycles)

Kristjánsson JE, McInnes H (1999) The impact of greenland on cyclone evolution in the North Atlantic. QJR Meteorol Soc 125:2819–2834

Levitus S (1982) Climatological atlas of the world ocean. In: NOAA/ERL GFDL professional paper 13. Princeton University Press, NTIS PB83–184093, pp 173

Li X (1999) Ensemble atmospheric GCM simulations of climate interannual variability from 1979 to 1994. J Clim 12:986–1000

Lott F, Miller MJ (1997) A new subgrid-scale orographic drag parameterisation: its formulation and testing. QJR Meteorol Soc 123:101–127

Loutre MF (1995) Greenland ice sheet over the next 5,000 years. Geophys Res Lett 22:783–786

Loutre MF, Kageyama M (2003) Continuous climate evolution scenarios over western Europe (1000 km scale). Deliverable D7, BIOCLIM project, EC-CONTRACT : FIKW-CT-2000–00024. Available from ANDRA—Agence Nationale pour la Gestion des Dechets Radioactifs Direction Scientifique—Service Milieu Geologique (DS/MG) Parc de la Croix Blanche—1–7, rue Jean Monnet 92298 Chatenay-Malabry Cedex, France (http://www.andra.fr/bioclim)

Lunt DJ, de Noblet-Ducoudré N (2003) Global climate characteristics, including vegetation and seasonal cycles over Europe, for snapshots over the next 200,000 years. Deliverable D4/5, BIOCLIM project, EC-CONTRACT: FIKW-CT-2000–00024. Available from ANDRA—Agence Nationale pour la Gestion des Dechets Radioactifs Direction Scientifique—Service Milieu Geologique (DS/MG) Parc de la Croix Blanche—1–7, rue Jean Monnet 92298 Chatenay-Malabry Cedex, France (http://www.andra.fr/bioclim)

Madec G, Delecluse P, Imbard M, Levy C (1999) In: OPA8.1 ocean general circulation model reference manual. Notes du pole de modelisation, Institut Pierre Simon Laplace des sciences de l'environnement global. LODYC, Paris

Marsh R, Gulamali M, Krznaric M, Newhouse S, Edwards NR, Lenton TM, Shepherd JG, Valdes PJ (2003) Multiple equilibria of the thermohaline circulation under anomalies in zonal and meridional moisture transport: early results with a new earth system model', poster presented at at EGS-AGU-EUG, Nice

Morcrette JJ (1991) Radiation and cloud radiative properties in the ECMWF operational weather forecast model. J Geophys Res 96:9121–9132

New M, Hulme M, Jones PD (1999) Representing twentieth century space-time climate variability. Part 1: development of a 1961–90 mean monthly terrestrial climatology. J Clim 12:829–856

Ohmura A, Reeh N (1991) New precipitation and accumulation maps for Greenland. J Glaciol 37:140–148

Petersen GN, Kristjánsson JE, Ólafsson H (2004) Numerical simulations of Greenland's impact on the northern Hemisphere winter circulation. Tellus A 56:102–111

Raymoa ME, Granta B, Horowitza M, Rau GH (1996) Mid-Pliocene warmth: stronger greenhouse and stronger conveyor. Mar Micropaleontol 27:313–326

Rind D (1987) Components of the ice age circulation. J Geophys Res 92:4241–4281

Ritz C, Fabre A, Letreguilly A (1997) Sensitivity of a Greenland ice sheet model to ice flow and ablation parameters: consequences for the evolution through the last glacial cycle. Clim Dyn 13:11–24

Tiedtke M (1989) A comprehensive mass flux scheme for cumulus parameterisation in large scale models. Monthly Weather Rev 117:1779–1800

Toniazzo T, Gregory JM, Huybrechts P (2004) Climatic impact of a Greenland deglaciation and its possible irreversibility. J Clim 17:21–33

Viovy N, de Noblet N (1997) Coupling water and carbon cycle in the biosphere. Sci Géol Bull 50(1–4):109–121

Xie P, Arkin PA (1997) Global precipitation: a 17-year monthly analysis based on guage observations, satellite estimates, and numerical model outputs. Bull Am Meteorol Soc 78:2539–2558